GENERAL STRUCTURE OF INTEGRATOR-BASED CONTINUOUS-TIME ACTIVE-RC FILTER AND APPLICATIONS

Slawomir Koziel,
Faculty of Electronics, Telecommunications and Informatics, Gdansk University of Technology, Gdansk, Poland
koziel@ue.eti.pg.gda.pl

DOI: 10.36724/2664-066X-2021-7-6-8-13

ABSTRACT

In the paper, a general structure of integratorbased continuous-time Active-RC filter is presented. More specifically, filter structures containing inverting amplifiers and passive feedback network are considered. The structure is analyzed using matrix description. The extensions of the model that take into account finite DC gain and finite bandwidth of operational amplifiers as well as other non-ideal effects are presented. The matrix-based approach is formulated especially for efficient use in computer-aidedanalysis and design of Active-RC filters. An application example of the proposed approach to obtain OPAMP specifications for 3rd order low-pass Chebyshev filter for Analog Front End for VDSL is given. In this paper, we consider a general Active-RC filter topology suitable for computer-aided analysis, design and optimization of Active-RC filters. The structure is not the most general one, since it is restricted to filter topologies containing only inverting amplifiers (especially integrators) and RC feedback network.

KEYWORDS: *RContinuous-time filters, Active-RC filters.*

The article is reworked from unpublished 2nd IEEE International Conference on Circuits and Systems for Communications (ICCSC) materials.

Introduction

Continuous-time analog filters based on operational amplifiers (OPAMPs) and RC elements (Active-RC filters) provide solutions for various signal-processing tasks. Many synthesis and design methods for different types and architectures of this class of filters have been reported [1],[2]. Although other techniques, particularly transconductance-capacitor (OTA-C) filters [3], are now dominant in high-frequency range, Active-RC filters are suitable for numerous medium-frequency applications, especially those which require high linearity and low noise, such as ADSL [4], VDSL [5], WCDMA [6],[7], RFIC receivers for PANs [8], GSM baseband transmitters [9]. Recently, an Active-RC filter for frequencies beyond 100MHz has been successfully implemented [10].

In this paper, we consider a general Active-RC filter topology suitable for computer-aided analysis, design and optimization of Active-RC filters. The structure is not the most general one, since it is restricted to filter topologies containing only inverting amplifiers (especially integrators) and RC feedback network. Thus, it is not suitable for analyzing some classical structures such as Sallen-Key biquad [2]. However, it covers a number of practical Active-RC filters, especially most multiple-loop feedback topologies including filters based on RLC ladder simulation, leap-frog, follow-the-leader [1]-[3], and makes it possible to generate and investigate new filter topologies with possibly attractive properties.

Integra-based Active-RC filter structure

Figure 1 shows the single-ended version of the general topology of integrator-based Active-RC filter. The filter in Fig.1 contains n operational amplifiers denoted as O_i, i=1,...,n, n input resistors R_{bi} and capacitors C_{bi}, i=1,...,n, the set of internal feedback resistors R_{ij} and capacitors C_{ij}, i,j=1,...,n, as well as output summer consisting of amplifier O_o, resistors R_d (direct feedforward path from input), R_{ci}, i=1,...,n and R_o. Output nodes of OPAMPs are denoted as x_i, i=1,...,n. We also use z_i (x_i) to denote voltages at OPAMP input (output) nodes. Any integrator-based Active-RC filter is a particular case of the structure in Fig.1 (after removing unnecessary elements). In this section we assume operational amplifiers to be ideal.

To start the analysis note that the total current flowing into each node z_i, i=1,...,n is zero and the voltage at z_i is also zero, due to assumed ideality of OPAMP. This allows us to write the following equations:

$$y_{bi}U_{in} + \sum_{j=1}^{n} y_{ij}x_j = 0\,, \quad i=1,...,n \qquad (1)$$

$$g_oU_{out} + \sum_{j=1}^{n} g_{cj}x_j + g_dU_{in} = 0 \qquad (2)$$

where U_{in} and U_{out} denote Laplace transforms of input and output voltages, respectively, and

$$y_{bi}=g_{bi}+sC_{bi}, \quad g_{bi}=1/R_{bi}, \quad i=1,...,n$$

$$g_{ci}=1/R_{ci}, \quad i=1,...n, \quad g_d=1/R_d, \quad g_o=1/R_o \qquad (3)$$

$$y_{ij} = g_{ij} + sC_{ij}\,, \quad g_{ij} = 1/R_{ij}\,, \quad i,j=1,...,n \qquad (4)$$

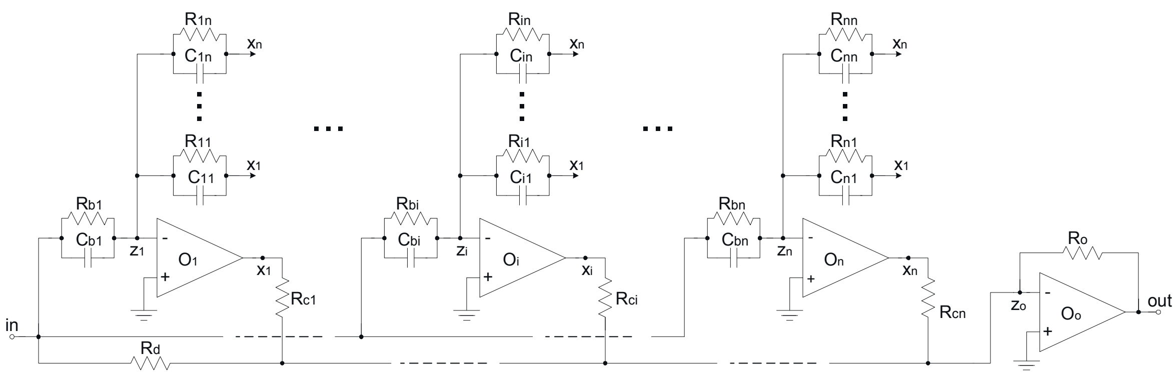

Fig.1. General structure of integrator-based Active-RC filter

Let us introduce the following notation

$$\boldsymbol{T}=\left[C_{ij}\right]_{i,j=1}^{n},\quad \boldsymbol{G}=\left[g_{ij}\right]_{i,j=1}^{n},\quad \boldsymbol{X}=\left[x_1\ \cdots\ x_n\right]^T$$

$$\boldsymbol{C}=\left[c_1\ \cdots\ c_n\right]=\left[g_{c1}/g_o\ \cdots\ g_{cn}/g_o\right], \tag{5}$$

$$\boldsymbol{B}=\left[g_{b1}+sC_{b1}\ \cdots\ g_{bn}+sC_{bn}\right]^T,\quad \boldsymbol{D}=d=g_d/g_o$$

Using (5) we can rewrite (1), (2) in the following form

$$(s\boldsymbol{T}+\boldsymbol{G})\boldsymbol{X}+\boldsymbol{B}U_{in}=0 \qquad U_{out}+\boldsymbol{CX}+\boldsymbol{D}U_{in}=0 \tag{6}$$

This allows us to calculate the transfer function $H(s)$ of the filter

$$H(s)=U_{out}(s)/U_{in}(s)=\boldsymbol{C}(s\boldsymbol{T}+\boldsymbol{G})^{-1}\boldsymbol{B}-\boldsymbol{D} \tag{7}$$

Now, let us denote adjoint matrix of $s\boldsymbol{T}+\boldsymbol{G}$ as $\boldsymbol{A}$ where

$$\boldsymbol{A}(s)=adj(s\boldsymbol{T}_C+\boldsymbol{G})=\left[A_{ij}(s)\right]_{i,j=1}^{n} \tag{8}$$

This allows us to rewrite transfer function in the form:

$$H(s)=\frac{1}{\det(s\boldsymbol{T}+\boldsymbol{G})}\sum_{i,j=1}^{n}c_i\left(g_{bj}+sC_{bj}\right)A_{ij}(s)-d \tag{9}$$

Note that in many filter structures, input signal is provided to only one internal node, say z_k (i.e. there is no input signal distribution), and there is no output summer (i.e. one of the internal nodes, say x_l, is the output of the filter), and no input capacitors. This means that $\boldsymbol{B}=\left[0\ \cdots\ 0\ \ g_{bk}\ \ 0\ \cdots\ 0\right]^T$, $\boldsymbol{C}=\left[0\ \cdots\ 0\ -1\ \ 0\ \cdots\ 0\right]$

with 1 at l-th position and $C_{bi}=0$ for $i=1,...n$ (note that we have -1 because of the fact that if there is no output summer, there is no signal inversion due to O_o either). In such a case, expression (9) reduces to the form:

$$H(s)=-g_{bk}A_{lk}(s)/\det(s\boldsymbol{T}+\boldsymbol{G}) \tag{10}$$

Similar expression can be written for more general cases.

On the basis of the above expressions one can easily calculate the transfer function of any particular structure of integrator-based Active-RC filter. It is also worth noting that there is one-to-one correspondence between integrator-based Active-RC filters and matrices (5). Thus, using presented matrix description we can consider filter design, analysis and optimization in purely algebraic domain. The main advantage is that this can be easily handled by a suitable computer software.

It follows that the order n_H of transfer function of general filter structure in Fig.1 is not necessarily equal to the number of internal nodes. It can be shown that it essentially depends on the passive network. In particular, we have that n_H is not larger than the rank of the corresponding matrix $\boldsymbol{T}$.

Based on the algebraic properties of the matrix $\boldsymbol{T}$, we can distinguish an important subclass of integrator-based Active-RC filters, i.e. state-space filters. If the matrix $\boldsymbol{T}$ is invertible, i.e. $\boldsymbol{T}^{-1}$ exists. Then we can rewrite (6) as

$$s\boldsymbol{X}=-\boldsymbol{T}^{-1}\boldsymbol{GX}-\boldsymbol{T}^{-1}\boldsymbol{B}U_{in} \qquad U_{out}=-\boldsymbol{CX}-\boldsymbol{D}U_{in} \tag{11}$$

Let us denote

$$\boldsymbol{A}_s=-\boldsymbol{T}^{-1}\boldsymbol{G},\quad \boldsymbol{B}_s=-\boldsymbol{T}^{-1}\boldsymbol{B},\quad \boldsymbol{C}_s=-\boldsymbol{C},\quad \boldsymbol{D}_s=-\boldsymbol{D} \tag{12}$$

With this notation (11) takes the form

$$s\boldsymbol{X}=\boldsymbol{A}_s\boldsymbol{X}+\boldsymbol{B}_s\boldsymbol{U}_{in} \qquad U_{out}=\boldsymbol{C}_s\boldsymbol{X}+\boldsymbol{D}_sU_{in} \tag{13}$$

which is the state-space description of the filter in Figure 1 with node voltages x_i, $i=1,...,n$ being the state variables. Thus, the state-space Active-RC filter is the one for which the matrix $\boldsymbol{T}$ is invertible which is a necessary and sufficient condition for the existence of the state matrices.

For state-space filters we can apply many useful matrix transformations which can be used, for example, to perform efficient parameter optimization [11].

In practice Active-RC filters are mostly implemented in fully differential structures. Due to this we may assume that matrix entries in (5) can take both positive and negative values, which can be accomplished by cross-coupling of corresponding physical elements. More specifically, if the element, say R_{ij}, is cross-coupled (i.e. put between positive [negative] output of an amplifier and positive [negative] input of another one, see e.g. resistor R_1 in Fig.2), this reflects in equation (1) so that the appropriate term has the form $g_{ij}(-x_j)=-g_{ij}x_j$, i.e. the original '-' from node voltage is moved into filter element, here g_{ij}. Obviously, the physical element remains positive. Negative value of the corresponding matrix entry is equivalent to cross-coupling. In case of single-ended implementation, negative elements must be realized using inverters.

The presented approach is primarily intended to be used as a basis for creating computer-aided design and optimization software. However, let us consider a simple example as an illustration how it can be used for hand design. Suppose that we want to synthesize an all-pole biquad filter, i.e. implement the transfer function:

$$H(s)=\frac{H_o\omega_0^2}{s^2+(\omega_0/Q)s+\omega_0^2} \tag{14}$$

If one wants to develop minimal implementation, two OPAMPs are needed, so we have n=2 in formulas (1)-(9). Assume that our filter has no input signal distribution with input signal injected to the first OPAMP through conductance g_b, i.e. $\boldsymbol{B}=[g_b\ 0]^T$, and no output summer with output signal taken from the second OPAMP, i.e. $\boldsymbol{C}=[0\ -1]$ and $\boldsymbol{D}$. Now we have to choose matrices $\boldsymbol{T}$ and $\boldsymbol{G}$ having in mind that in our case the transfer function of the filter is given by (10). More specifically, denominator of the transfer function is just $\det(s\boldsymbol{T}+\boldsymbol{G})$, while its numerator is $g_bA_{21}(s)$, where $A_{21}(s)=-[s\boldsymbol{T}+\boldsymbol{G}]_{21}$, i.e. element $_{21}$ of the matrix $s\boldsymbol{T}+\boldsymbol{G}$ (multiplied by -1). There are still many possibilities, but the simplest choice is

$$\boldsymbol{T}=\begin{bmatrix}C_1 & 0\\ 0 & C_2\end{bmatrix},\qquad \boldsymbol{G}=\begin{bmatrix}0 & -g_1\\ g_2 & g_3\end{bmatrix} \tag{15}$$

which gives all-pole second-order transfer function:

$$H(s)=\frac{g_bg_2}{s^2C_1C_2+sC_1g_3+g_1g_2}=\frac{g_bg_2/C_1C_2}{s^2+s\,g_3/C_2+g_1g_2/C_1C_2} \tag{16}$$

Corresponding filter topology (in fully differential structure) is shown in Fig.2. Obviously, we can obtain many more equivalent filter topologies that implement transfer function (14) by different choice of matrices ***T***, ***G***, ***B***, ***C*** and ***D***.

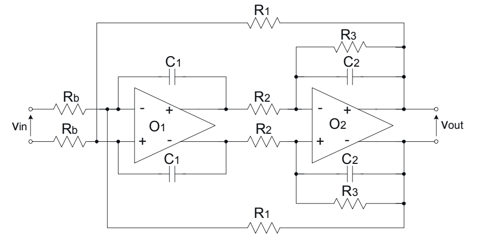

Fig.2. Active-RC biquad corresponding to matrices (15)

III. Active-RC filter with non-ideal OPAMPs

In this section we extend the model presented above to take into account non-ideal behavior of OPAMPs. We shall consider finite gain-bandwidth product of OPAMP as well as its non-zero output resistance. In case of finite gain of OPAMP we can no longer assume that node voltages z_i, i=1,...,n are equal to zero. Denote the gain of i-th operational amplifier O_i as $A_i(s)$ as shown in Fig.3.

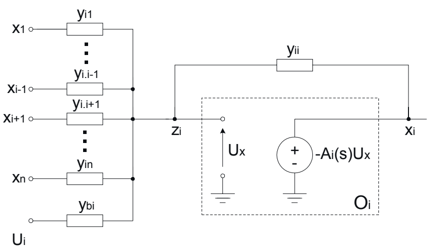

Fig.3. i-th integrator of the filter in Fig.1 with finite gain OPAMP

It follows from Fig.3 that i-th integrator of the filter can be described by the equations:

$$\begin{aligned} & y_{bi}(U_{in}-z_i)+\sum_{j=1}^{n} y_{ij}(x_j-z_i)=0 \qquad i=1,...,n \\ & x_i=-z_i A_i(s) \end{aligned} \tag{17}$$

The corresponding equations for the output summer are

$$\begin{aligned} & g_o(U_{out}-z_o)+\sum_{j=1}^{n} g_{cj}(x_j-z_o)+g_d(U_{in}-z_o)=0 \\ & U_{out}=-z_o A_o(s) \end{aligned} \tag{18}$$

where $A_o(s)$ is the gain of the operational amplifier O_o. Equations (17) and (18) can be rewritten in matrix form:

$$(s\boldsymbol{T}+\boldsymbol{G}+\boldsymbol{Y}_A)\boldsymbol{X}+\boldsymbol{B}U_{in}=0 \qquad (1+C_A)U_{out}+\boldsymbol{C}\boldsymbol{X}+\boldsymbol{D}U_{in}=0 \tag{19}$$

where

$$\boldsymbol{Y}_A=\begin{bmatrix} \left(\sum_{j=1}^{n}\bar{y}_{1j}+\bar{y}_{b1}\right)/A_1(s) & & 0 \\ & \ddots & \\ 0 & & \left(\sum_{j=1}^{n}\bar{y}_{nj}+\bar{y}_{bn}\right)/A_n(s) \end{bmatrix} \tag{20}$$

$$C_A=\left(1+\sum_{j=1}^{n}\bar{c}_j+\bar{d}\right)/A_o(s) \quad (C_A=0 \text{ if there is no output summer}) \tag{21}$$

Here, $\bar{y}_{bi}=|g_{bi}|+s|C_{bi}|$, $\bar{y}_{ij}=|g_{ij}|+s|C_{ij}|$, $\bar{c}_i=|c_i|$, i,j=1,...,n, $\bar{d}=|d|$, which allows us to take into consideration the case when some entries of the matrices ***T***, ***G***, ***B***, ***C***, ***D*** are negative. In such a case (which is equivalent to cross-coupling of the corresponding physical elements), negative sign of the element value corresponds in fact to the negative sign of appropriate node voltage x_j (see discussion in Section 2). However, from the point of view of input node voltage z_i element is still positive and we must take absolute value of negative elements to maintain correctness of equations. Using (19) we can calculate transfer function of the filter, which is:

$$H(s)=(1+C_A)^{-1}\left(\boldsymbol{C}(s\boldsymbol{T}+\boldsymbol{G}+\boldsymbol{Y}_A)^{-1}\boldsymbol{B}-\boldsymbol{D}\right) \tag{22}$$

Note that even if $A_i(s)$ is modeled using single pole approximation, matrix elements of $\boldsymbol{Y}_A$ are, in general, of second order in s. This makes it difficult to directly evaluate the transfer function formula (22). However, if for frequencies of operation of the filter we have $|A_i(s)|>>1$, i=1,...,n, $|A_o(s)|>>1$, which means that $\|\boldsymbol{Y}_A\|<<\|s\boldsymbol{T}+\boldsymbol{G}\|$ for any reasonable matrix norm, we can use the approximation $(\boldsymbol{I}+\boldsymbol{A})^{-1}\approx\boldsymbol{I}-\boldsymbol{A}$ which is valid for any matrix $\boldsymbol{A}$ as far as $\|\boldsymbol{A}\|<<\|\boldsymbol{I}\|$ (***I*** stands for an identity matrix). Using this we obtain the following formula:

$$H(s)\cong(1+C_A)^{-1}H_0(s)-\Delta H(s) \tag{23}$$

where $H_0(s)$ is the nominal transfer function of the filter with ideal OPAMPs (cf. (7)), and $\Delta H(s)$ is deviation from $H_0(s)$ due to finite OPAMP gains given by

$$\Delta H(s)=(1+C_A)^{-1}\boldsymbol{C}(s\boldsymbol{T}+\boldsymbol{G})^{-1}\boldsymbol{Y}_A(s\boldsymbol{T}+\boldsymbol{G})^{-1}\boldsymbol{B} \tag{24}$$

Now, we shall consider the effect of non-zero output impedance of the filter OPAMPs. Fig.4 shows i-th OPAMP of the filter, where $y_{oi}=1/z_{oi}$ denotes its output admittance, $\tilde{x}$ and x_i are the internal and external output voltages of the OPAMP, respectively.

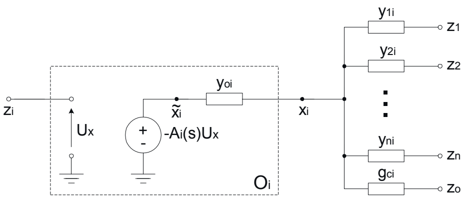

Fig.4. Diagram of *i*-th OPAMP of the filter in Fig.1 with non-zero output admittance

Since in practice we always have $|z_j| << |x_i|$, $i,j=1,...,n$, we can write the following equation:

$$\left(\widetilde{x}_i - x_i\right) y_{oi} = x_i \left(| g_{ci} | + \sum_{j=1}^{n} \bar{y}_{ji} \right), \quad i=1,...,n \qquad (25)$$

where we wrote $|g_{ci}|$ and $\bar{y}_{ji}$ for the same reason as in (20). Hence, we have

$$x_i = \widetilde{x}_i \frac{y_{oi}}{y_{oi} + | g_{ci} | + \sum_{j=1}^{n} \bar{y}_{ji}}, \quad i=1,...,n \qquad (26)$$

This means that effective gain of the amplifier is reduced by the factor $\left(1 + z_{oi}\left(| g_{ci} | + \sum_{j=1}^{n} \bar{y}_{ji} \right)\right)^{-1}$, which is, in general, frequency dependent. In order to take it into account output in our previous formulas, we have to replace $A_i(s)$ in (21) by $\widetilde{A}_i(s)$ given by

$$\widetilde{A}_i(s) = A_i(s) \Big/ 1 + z_{oi}\left(| g_{ci} | + \sum_{j=1}^{n} \bar{y}_{ji} \right) \qquad (27)$$

In a similar way, one can treat output impedance of O_o - OPAMP of the output summer of the filter. We have

$$\left(\widetilde{U}_{out} - U_{out}\right) y_o = U_{out} \, | g_o |, \qquad (28)$$

where $\widetilde{U}_{out}$ and U_{out} are internal and external output voltages of O_o, while $y_o = 1/z_o$ is its output admittance. Hence, we get

$$U_{out} = \widetilde{U}_{out} \, y_o / \left(y_o + | g_o |\right), \qquad (29)$$

which results in replacing $A_o(s)$ in (20) by $\widetilde{A}_o(s)$:

$$\widetilde{A}_o(s) = A(s) / \left(1 + z_o \, | g_o |\right) \qquad (30)$$

IV. Application example

As an application example of the proposed model we shall obtain OPAMP specifications for 3rd order low-pass 1dB Chebyshev filter (3dB frequency equal to 12MHz) for VDSL Analog Front End [5]. Design specifications for VDSL filters are very tough, especially with respect to noise and linearity. Here, we are merely interested in transfer function distortion due to finite gain-bandwidth product and output resistance of filter OPAMPs. We shall consider leap-frog topology shown in Fig.5. We assume that all resistors in the filter are the same and equal to the common value R. We aim at estimating required OPAMP gain-bandwidth product (GBW) and output resistance r_o so that distortion of the filter transfer function due to these non-idealities is within acceptable range.

Fig.6 shows ideal frequency response of the filter in Fig.5, and the response for GBW of OPAMP equal to 200MHz and r_o/R=0.5. We can observe both amplitude distortion (picking) ΔA and 3dB frequency error Δf_{3dB}. Figs.7 and 8 show ΔA and Δf_{3dB}, respectively, versus GBW of OPAMP, for different values of the ratio r_o/R. All the results have been obtained in a single run of the Matlab program implementing formulas presented in Sections II and III. It is seen that Δf_{3dB} is not a big problem since its value is relatively small and can be easily compensated by calibration. However, ΔA is large and heavily dependent on both GBW and r_o/R.

Table 1 shows the value of GBW required to keep ΔA<2dB for different r_o/R ratios. The data in Table 1 represents trade-off between GBW and r_o of the OPAMP. Although we can relax requirements concerning GBW it is always at the expense of decreasing r_o/R ratio. It is not possible to keep this ratio small just by increasing resistor value R because this results in increasing filter noise, which is undesirable. Thus, we have an alternative: either try to obtain large GBW or decrease OPAMP output resistance (this, however, influences OPAMP architecture - very small values of r_o can only be obtained using output buffer which, in turn, degrades both circuit linearity and frequency performance). Discussion of this problem is, however, beyond the scope of this paper. Our goal was just to estimate GBW and r_o/R for which the transfer function distortion is under desired level.

Table 1. OPAMPs GBW ensuring ΔA<2dB of the filter in Fig.5

r_o/R	0	0.25	0.5	1.0	1.5
GBW [MHz]	165	350	550	970	1400

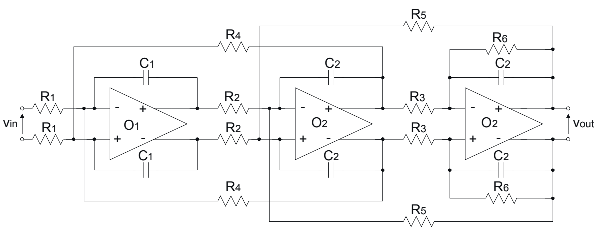

Fig.5. Fully differential 3rd order leap-frog Active-RC filter

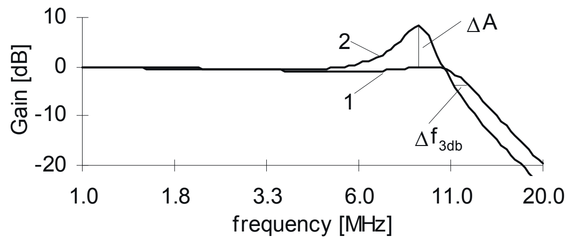

Fig.6. Transfer function distortion of the filter in Fig.5 due to finite OPAMP GBW and r_o; ideal (1) and actual (2) response

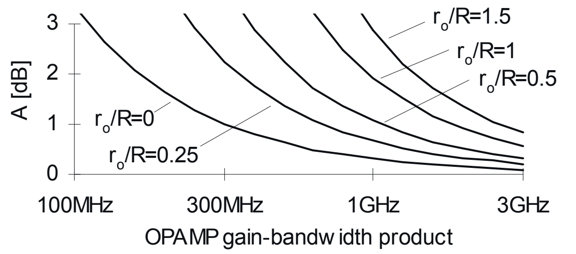

Fig.7. Amplitude distortion ΔA versus GBW of filter OPAMPs for different values of r_o/R ratio

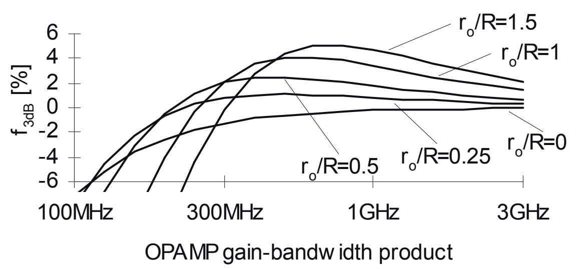

Fig.8. Corner frequency error Δf_{3dB} versus GBW of filter OPAMPs for different values of r_o/R ratio

V. Conclusions

A general structure of integrator-based Active-RC filter is introduced and analyzed using algebraic description. As a result, a matrix-based framework for creating efficient computer-aided analysis and design tools for Active-RC filters is developed. The goal of the future work is to develop, within the presented approach, tools for evaluating noise and nonlinear effects in Active-RC filters and use them in automated design/optimization system.

References

[1] R. Schaumann, M. S. Ghausi, and K. R. Laker, *Design of Analog Filters, Passive, Active RC, and Switched Capacitor*. Englewood Cliff, NJ: Prentice-Hall, 1990.

[2] K. Su, *Analog Filters*, Kluwer Academic Publishers, 2002.

[3] Y. Sun (Editor), *Design of high frequency integrated analogue filters*, The Institution of Electrical Engineers, London, 2002.

[4] S.-S. Lee, „Integration and System Design Trends of ADSL Analog Front Ends and Hybrid Line Interfaces”, *Proc. IEEE Custom Integrated Circuits Conf.*, pp.37-44, 2002.

[5] H. Weinberger, A. Wiesbauer, M. Clara, C. Fleischhacker, T. Potscher, B. Seger, „A 1.8V 450mW VDSL 4-Band Analog Front End IC in 0.18µm CMOS”, *Proc. IEEE Solid-State Circuits Conf. ISSCC*, Vol.1, pp.326-471, 2002.

[6] J. Jussila, K. Halonen, „A 1.5 V active RC filter for WCDMA applications”, *Proc. IEEE Int. Conf. Electronics Circuits. Syst. ICECS*, Vol.1, pp.489-492, 1999.

[7] W. Khalil, T.-Y. Chang, X. Jiang, S.R. Naqvi, B. Nikjou, J. Tseng, „A highly integrated analog front-end for 3G”, *IEEE J. Solid-State Circuits*, Vol.38, pp.774-781, 2003.

[8] C. Frost, G. Levy, B. Allison, „A CMOS 2MHz self-calibrating bandpass filter for personal area networks”, *Proc. Int. Symp. Circuits Syst. ISCAS*, Vol.1, pp.485-488, 2003.

[9] C.S. Wong, „A 3-V GSM baseband transmitter”, *IEEE J. Solid-State Circuits*, Vol.34, pp.725-730, 1999.

[10] J. Harrison, N. Weste, „350MHz opamp-RC filter in 0.18µm CMOS”, *Electron. Lett.*, Vol.38, pp.259-260, 2002.

[11] S. Koziel, S. Szczepanski, R. Schaumann, „General Approach to Continuous-Time G_m-C Filters”, *Int. J. Circuit Theory Appl.*, Vol.31, pp.361-383, July/Aug. 2003.